

Identification of buried sinkholes using refraction tomography at Ft. Campbell Army Airfield, Kentucky

I. Camilo Higuera-Díaz · Philip J. Carpenter ·
Michael D. Thompson

Received: 16 October 2006 / Accepted: 13 February 2007 / Published online: 7 March 2007
© Springer-Verlag 2007

Abstract Karst aquifers are highly susceptible to contamination, with numerous points of entry for contaminants through recharge features such as sinkholes, swallow holes and solutionally enlarged fractures. These recharge features may be filled or obscured at the surface, requiring the use of geophysical or remote sensing techniques for their identification. This study uses seismic refraction data collected at the Ft. Campbell Army Airfield (CAAF), Kentucky, USA, to test the hypothesis that refraction tomography is a useful tool for imaging bedrock depressions beneath thick overburden (greater than 20 m of unconsolidated sediment). Southeast of the main taxiway of CAAF seismic velocity tomograms imaged a bedrock low, possibly a closed depression, at a depth of 25 m that had been earlier identified through delay-time analysis of the same refraction data. Tomography suggests the bedrock low is about 250-m wide by 10-m deep at its widest point. High rates of contaminant vapor extraction over the western extension of this feature suggest a high concentration of contaminants above, and within, this filled bedrock low, the base of which may contain solutionally enlarged fractures (i.e. karst conduits) that could funnel these contaminants to the upper or lower bedrock aquifers. This study thus demonstrates the viability of seismic refraction tomography as a tool for identification of filled sinkholes and bedrock depressions in karst areas.

Keywords Geophysics · Ground water · Carbonate hydrology

Introduction

Karst systems pose unique challenges to contaminant characterization and remediation. Fracture and void systems within the rock provide conduits for migration of contamination, as do bedding plane partings and weathered zones. In areas where the karst is mantled by unconsolidated sediment and/or residuum, the topography of the karstic bedrock surface can be an important target for identifying points of contaminant infiltration and entrapment. Topographic lows in the karst surface provide a greater column of overburden and residuum in which to trap contaminants. However, these lows may also be associated with hydraulically transmissive zones where rocks have been preferentially weathered because they are fractured or contain solution openings. Contaminants that do manage to migrate through the thicker overburden might easily percolate to bedrock aquifers via these zones.

This paper explores the utility of seismic refraction tomography in characterizing buried karst topography in an urban and/or industrial setting where electrical or electromagnetic methods would likely fail. Specifically, this study tests the hypothesis that seismic refraction tomography may be used to identify and image depressions in the bedrock surface, even when they are buried by 20 m or more of unconsolidated sediment. Tomography also allows lateral velocity variations and vertical gradients to be imaged, as opposed to most conventional refraction interpretation methods, which require constant velocity layers.

I. C. Higuera-Díaz (✉) · P. J. Carpenter
Department of Geology and Environmental Geosciences,
Northern Illinois University, DeKalb IL 60115, USA
e-mail: ihiguera@niu.edu; higuera@geol.niu.edu

M. D. Thompson
Energy Systems Division, Argonne National Laboratory,
9700 S. Cass Avenue, Argonne, IL, USA

Physiographic and geological setting

Fort Campbell Army Airfield (CAAF) is located in the northeastern corner of Ft. Campbell, Kentucky, about 80 km northwest of Nashville, TN (Fig. 1). CAAF was originally built in 1942 to house an armored division and troops; it was made into an airfield in 1949, with the airfield covering approximately 810 ha.

CAAF lies on the southwest flank of the Cincinnati Arch, about 65 km east of the Mississippi Embayment. CAAF is underlain by unconsolidated deposits consisting primarily of residuum (likely derived from the St. Genevieve Limestone), which in turn, overlies karstified St. Genevieve and St. Louis Limestone. The unconsolidated deposits range in thickness from 5 to 45 m beneath CAAF and are 20–30 m thick in the vicinity of the study site.

Hydrogeology

A two-aquifer conceptual model has been proposed for CAAF. In this model the upper aquifer consists of discontinuous areas of saturation within the residuum and within the epikarst (weathered upper bedrock) zone. Vertical flow dominates the upper aquifer, which is

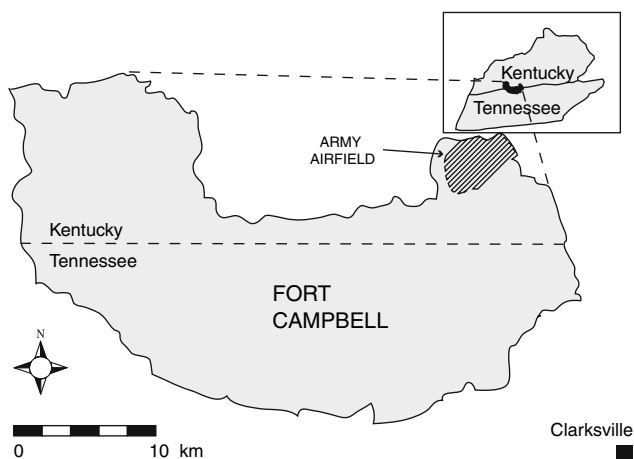
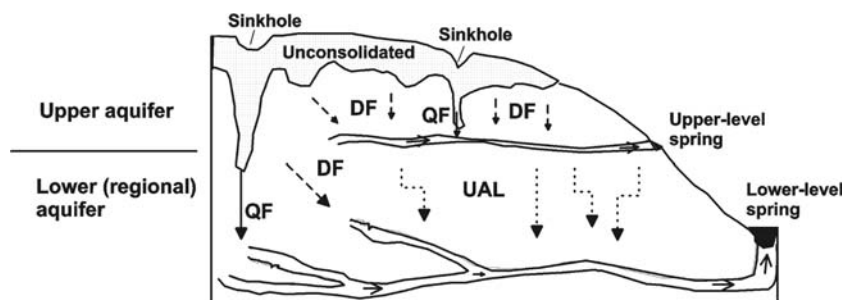


Fig. 1 Location of Fort Campbell, KY. The Fort Campbell Army Airfield (CAAF) is located in the northeast corner of this military reservation, with the plane runways oriented NE–SW

Fig. 2 Conceptual hydrogeological model of CAAF (after EWC 1994 and ADL 1997). DF is diffuse flow, UAL is upper aquifer leakage, and QF is quick-flow. The top of the lower aquifer is about 15–18-m deep on the left side of the figure

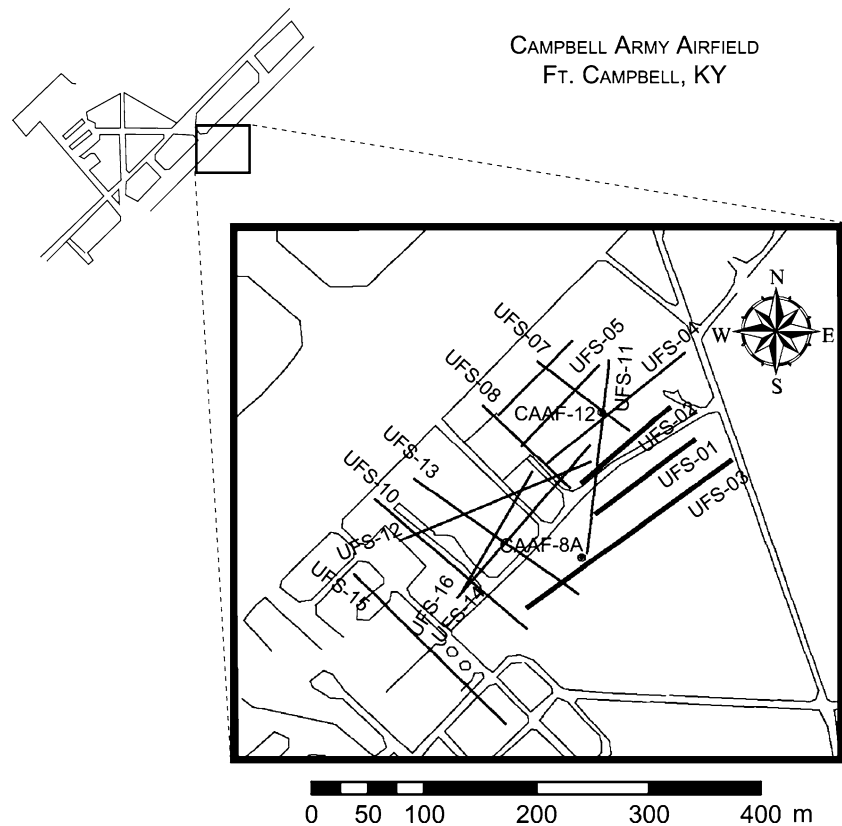


strongly influenced by seasonal precipitation patterns. Recharge occurs from diffuse flow through the residuum and epikarst, as well as quick-flow from conduits associated with sinkholes (Carey 1990). This upper aquifer discharges at seeps and “upper-level” springs (Carey 1990; ADL 1997; EWC 1997). ADL (1997) describes the upper aquifer as “limited spatially” and, in places, it “may be perched above the regional bedrock aquifer.” In contrast, the lower aquifer consists of a continuous zone of saturation within the bedrock with a potentiometric surface 15–18 m beneath the ground surface. This lower aquifer, referred to as the “regional bedrock aquifer” by ADL (1997) and Padar (1998), also has a potentiometric surface near the level of Little West Fork Creek, just west of the study area. This lower aquifer receives water through diffuse percolation from the surface, from losing streams, from slow leakage from the upper aquifer, and direct quick-flow recharge from the surface through sinkholes connected to karst conduits (i.e. solutionally enlarged fractures). These different flow paths are shown in the conceptual hydrogeological model in Fig. 2, which is based on over 10 years of dye tracing experiments and monitoring spring discharge (i.e. spring stages), spring water temperature, chemistry, electrical conductivity and turbidity changes (EWC 1989; Carey 1990; EWC 1994; ADL 1997; EWC 1997). For example, Fig. 3 shows results of dye tracing experiments that link the study area (near Sinkholes B and C) with a lower-level spring (Quarles Spring), approximately 4 km from the injection point. Quick-flow was observed during these experiments with ground-water velocity between the airfield and spring ranging from approximately 30–70 m/s, depending on the season (EWC 1989; ADL 1997). There is no evidence, however, for filled sinkholes directly linking the upper and lower aquifers. The left-most sinkhole in Fig. 2, for example, “bypasses” the upper aquifer (perhaps through an unsaturated area) and directly recharges the lower aquifer.

Soil and groundwater contamination

Soil contamination due to fuel leakage was first discovered at CAAF in 1982, with additional soil and deeper

Fig. 4 Map showing location of refraction survey lines at CAAF. The airfield corresponds to the enlarged shaded region in Fig. 1



of 5 m. Line UFS-03 was shot in two segments, so some shots in segment 2 were only offset 5–10 m from their locations in segment 1.

Data analysis

Refraction first arrival times for these three lines were initially analyzed using the delay time program SIPT1 (Haeni et al. 1987). Travel times for the three lines in the survey are shown in Fig. 5. Thompson et al. (1999) used a 3-layer undulating refractor model to interpret the travel times, with the deepest unit interpreted as bedrock. These results are summarized in Fig. 6, which shows contours depicting bedrock topography southeast of the CAAF runways. Travel-time plots and detailed delay-time models used to generate this contour map have been previously published in Thompson (1999), Thompson et al. (1999), Carpenter et al. (2003) and Carpenter et al. (2004).

The three lines chosen for tomographic inversion in this study target the eastern extent of this bedrock depression. UFS-01, UFS-02, and UFS-03 are parallel to each other and oblique to the long axis of the depression. Tomographic models were generated in this study in an attempt to improve upon the delay-time models and to verify the existence of the buried depression observed in the model of UFS-03. Tomographic models may also reveal lateral and vertical velocity variations that define subsurface structures

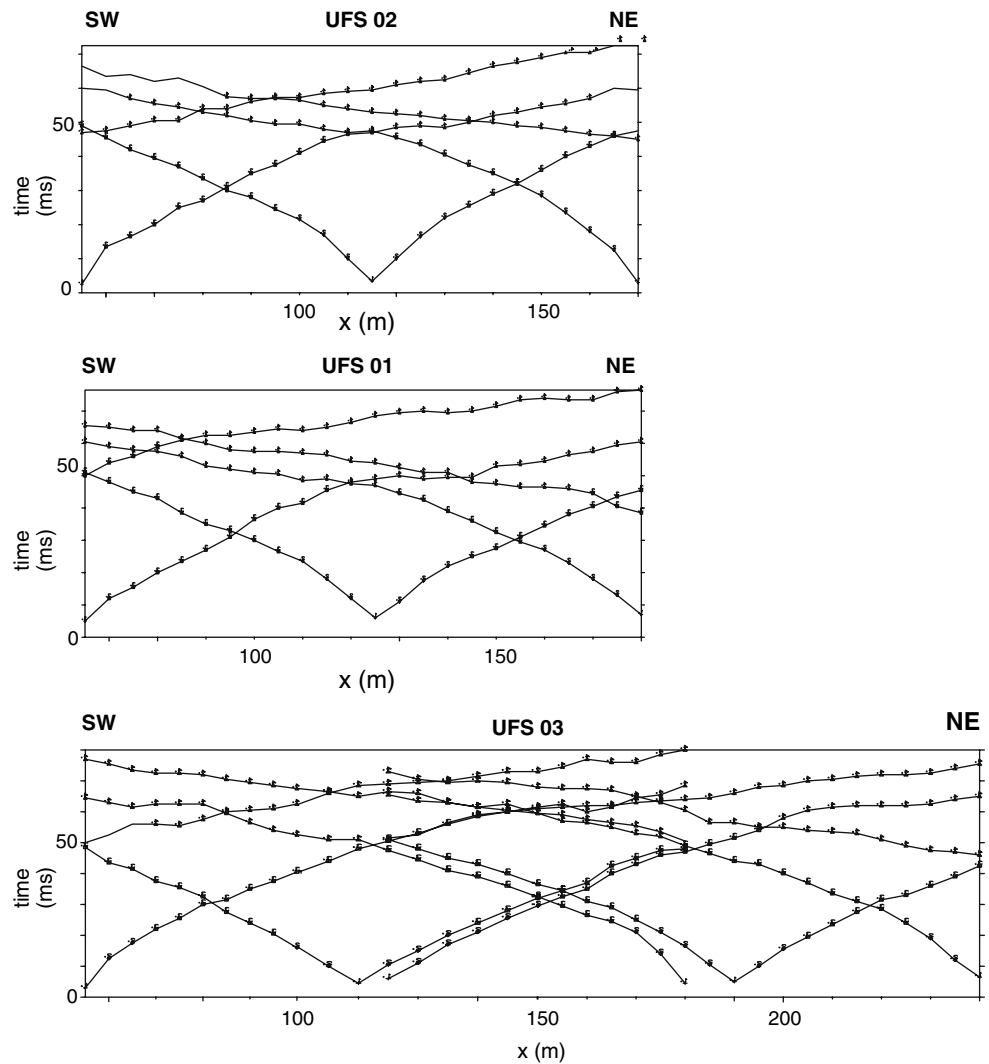
in a more realistic manner. Given sufficient data, tomographic modeling has the potential for better resolution of lateral and vertical velocity variations and imaging of irregular features (e.g. irregular bedrock topography) that could not be resolved by delay-time methods.

In this study traveltimes shown in Fig. 5 from lines UFS-01, UFS-02, and UFS-03 were inverted using the proprietary tomographic inversion code GeoCT-II, v 2.3 (GeoTomo LLC 2002). This code is based on the use of a non-linear least squares technique for the inversion process, and a wavefront propagation approach for the modeling of travel times (Zhang and Toksoz 1998). A unique aspect of the GeoCT-II inversion algorithm is that it seeks to minimize the difference between data and model values for both the average slowness (travel time divided by raypath length) and apparent slowness (slope of the travel-time curve), instead of just minimizing the misfit between modeled and observed travel times. The third unique aspect of the GeoCT-II program is that it utilizes Tikhonov regularization to minimize model “roughness” (Zhang and Toksoz 1998).

Results and discussion

In tomographic inversion, the initial step is to generate a theoretical velocity model that serves as the template (or

Fig. 5 Traveltimes for lines UFS-01, UFS-02, and UFS-03. Solutions are shown from *top to bottom* following the north–south location of the lines in the survey. For the location of these lines please see Fig. 4



initial model) to begin modeling traveltimes from the field data. The final tomographic inversion model depends heavily on the characteristics of the initial velocity template. The initial velocity template in this study was based on velocities obtained from the delay-time models of Thompson et al. (1999), as well as borehole data. Two main configurations were tested: a half space layered initial model, and a half space vertical linear velocity gradient. For both configurations different combinations of inversion parameters were tested, along with different numbers of iterations, until a stable model was obtained for each line that was consistent with the refraction field data and borehole geology. The results show that an initial model with a vertical linear velocity gradient fit the field and borehole data better, and produced more stable tomographic models.

This initial model had a surface velocity of 200 m/s and a velocity gradient of 200 (m/s)/m. This initial velocity

model was then used in the inversion of first arrival times from all three lines. After ten inversion iterations a velocity model was obtained for each line that shows bedrock topography, with vertical and lateral velocity changes as depicted in Fig. 7. The red contour, 4,000 m/s, is interpreted as bedrock since sonic logs from three wells located along the main runway at the CAAF suggest an upper bedrock velocity of 4,000 m/s (Thompson et al. 1999).

Line UFS-02 shows a more or less level bedrock surface. Lines UFS-01 and UFS-03, however, suggest broad lows exist in the bedrock surface. The tomogram for UFS-01 shows a well-defined low velocity region about 70-m wide and 5–10-m deep near the southwest edge of the line. This low in the bedrock surface could represent a northward extension of the large bedrock depression identified by the delay-time models. UFS-03 shows a much broader bedrock low, about 250-m wide, almost spanning the entire refraction line. The deepest portion of the interpreted

Fig. 6 Bedrock topography map based on delay time solutions from refraction lines and boring logs. The rectangle encloses lines used for the tomographic inversion in this study. Only a few deep borings are shown here—a large number of fuel extraction wells and other shallow borings located near UFS-12 and 14 are omitted for clarity

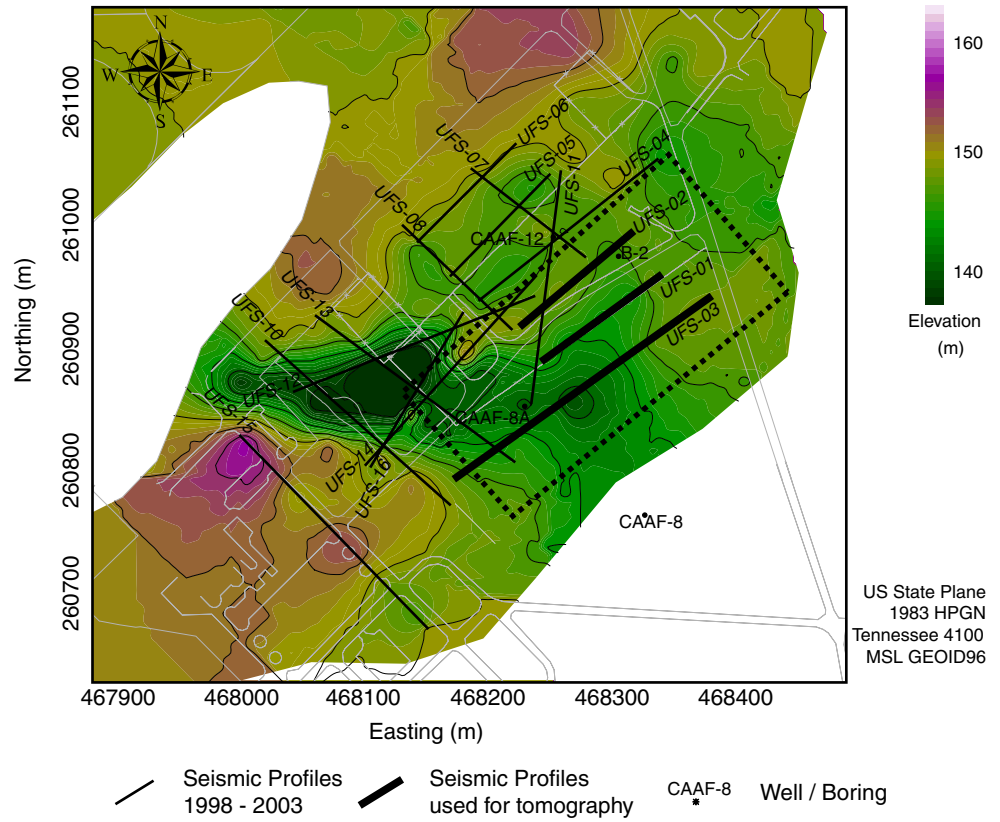
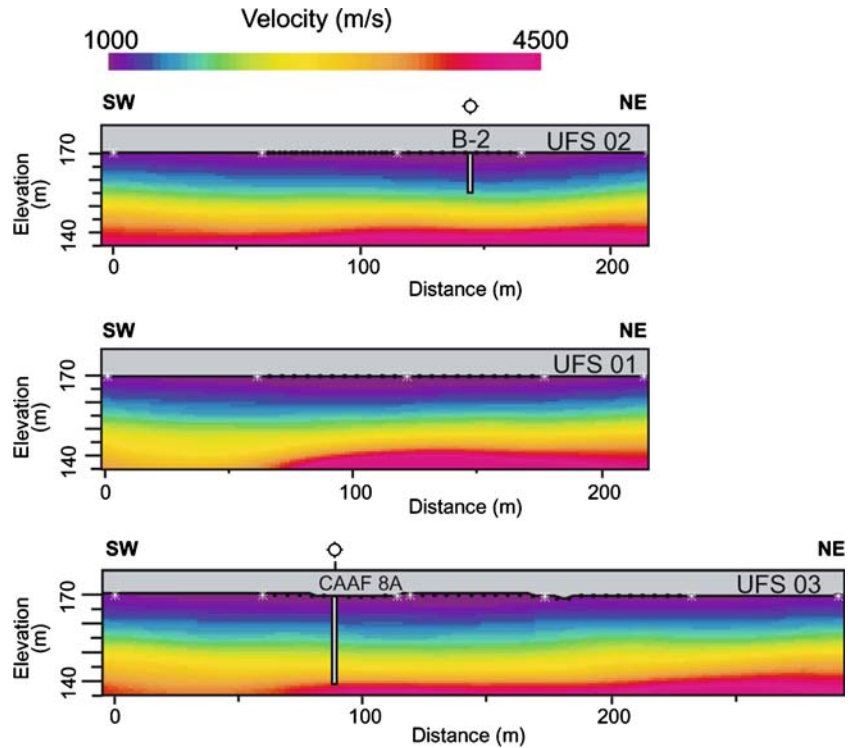


Fig. 7 Resulting tomographic velocity models after a ten-iteration inversion of the refraction travel times using program GeoCT-II. Projections of adjacent borings are also shown, extending to the interpreted top of bedrock. *White asterisks* represent shotpoints and *black dots* represent geophones. Tomographic models are displayed north to south as follows: **a** UFS-02, **b** UFS-01, and **c** UFS-03



bedrock is also on the southwest part of the line. This dip in the interpreted bedrock surface is about 50-m wide by 10-m deep.

Several criteria were used to evaluate the accuracy of these tomographic models including solution robustness and stability, comparisons with boring logs, and compari-

son with existing sinkholes visible at the surface. These criteria are briefly discussed in more detail below.

Solution robustness

Different parameter combinations and velocity constraints were tested for the inversions. The number of iterations was varied from 10 to 100. Significant model improvement, however, did not occur beyond ten iterations. After numerous tests the final tomography inversion with GeOCT-II utilized a smoothing parameter of 1.0, an X/Z smoothing scaling of 4.0, with an inversion grid ratio of X/Z of 2:1. The inversion grid ratio was found to be critical in providing stable, clear models. A large number of initial models were also tested involving velocities between 200 and 6,000 m/s. Gradient initial models produced much more realistic final models, as opposed to layered or half-space initial models.

Seismic refraction tomography contains very few assumptions, compared to conventional refraction processing, which makes tomography well-suited for imaging karst features. Sheehan et al. (2005) evaluated the validity of seismic refraction tomography in karst areas by examining eight models consisting of typical subsurface karstic structures. They found that tomography codes worked best with initial models containing velocity gradients, and in the case of models containing a buried bedrock depression, or bedrock low, such codes produced a velocity tomogram showing a smoothed depression, as well as (in some cases) a high-velocity artifact immediately beneath the depression. Models with broad epikarstal features (dimensions of 10 m or more), however, were faithfully reproduced in the seismic velocity tomograms. Sharp epikarstal features such as pinnacles, spires and caves, with lateral dimensions of only a few meters, were poorly resolved, and were associated with computational artifacts. The bedrock topographic depressions imaged in this study are all substantially wider than 10 m, and artifacts do not appear to be a major problem in the tomographic images.

Comparisons with surface sinkholes

Dozens of closed surface depressions control the topography in undeveloped areas surrounding CAAF. These probably represent numerous sinkholes and differential erosion along major fractures that coalesced into broad dolines, with dimensions 100–200 m across (Kemmerly 1976). These features are broad, shallow basins, with profiles very similar to the tomographic images of subsurface bedrock topography. Larger depressions, visible in digital elevation models (DEMs) derived from the 1/3 arc second National Elevation Dataset ([\[less.usgs.gov\]\(http://less.usgs.gov\)\), range from 100 to 400 m in diameter and can be as deep as 5 m below the surrounding plateau. This depth does not include the thickness of accumulated sediment within these depressions.](http://www.seam-</p>
</div>
<div data-bbox=)

Conventional topographic maps and geologic provide more detail and show internal drainage within these depressions. Some of the larger diameter topographic lows (up to 300-m wide and 5-m deep) have penetrated the St. Genevieve limestone and exposed the underlying St. Louis limestone (Klemic 1966). High-resolution topographic maps (ADL 1997) show depressions with internal drainage in undeveloped areas surrounding CAAF range in diameter from 50–200 m, and have maximum depths of about 3 m. Again, this depth does not include thickness of accumulated sediment. These dimensions are consistent with the dimensions of the bedrock lows on the tomographic images.

Comparisons with wells and borings

Boring CAAF 8A lies 15 m directly northwest of UFS-03. This boring may be within the elongate bedrock depression since it did not encounter bedrock, despite being over 30-m deep. Figure 7 suggests it ended just above the bedrock surface (perhaps when the driller encountered auger refusal).

The log from this boring describes the upper 15 m as a clayey silt soil with some sand and gravel, and the lower 15 m as a stiff lean clay with chert seams (Dames and Moore 1988). The water table is approximately 9-m deep, based on soil moisture levels (most likely this represents a saturated zone in the upper aquifer). Thus, the water table probably corresponds to the transition from the blue to green color in the UFS-03 tomogram. The green corresponds to saturated sediment velocities of 1,500–1,700 m/s. Boring B-2 lies 5 m southeast of UFS-02. This boring encountered unsaturated lean clay from the surface to the top of “very weathered” bedrock at 14-m depth, where auger refusal occurred (Dames and Moore 1989). Both the tomographic and delay-time models suggest bedrock is 15–20-m deep along UFS-02, considerably deeper than the boring log reports. One explanation for this inconsistency is that the drillers encountered a float block in the regolith and not “true” bedrock. Auger drilling would not be able to penetrate this block to verify its continuity. Another possibility is that that true bedrock was encountered, but in a highly weathered and unsaturated state its velocity is similar to that of unconsolidated material. Finally, a small bedrock pinnacle, or high, could have been encountered by the auger. Such a feature would not be resolved by the refraction tomography, which, at this site, can only resolve features that are 10 m or larger.

Discussion and conclusions

Refraction data obtained over buried karst features is often complex, requiring sophisticated analysis and interpretation techniques. This study suggests tomographic inversion may be used to image bedrock surfaces containing buried depressions below as much as 25 m of unconsolidated overburden. The use of such programs needs to be considered carefully, however. Tomographic imaging programs require a great deal of user intervention and experience to use effectively. For example, combinations of parameters in the inversion module need to be chosen carefully, otherwise the model and inversion process will become unstable. With the GeoCT-II codes used in this study, velocity models must also be extended beyond the edges of the refraction line, as well as above the earth's surface, and various initial models need to be tested. For this data set, which was not originally collected for tomographic inversion, optimum results were obtained utilizing a smoothing parameter of 1.0, an X/Z smoothing scaling of 4.0, with an inversion grid ratio of X/Z of 2:1. In any type of tomographic inversion the interpreter must have a strong understanding of viable solution types, and outside information is required to confirm the model results.

In this study a large elongate buried bedrock low southeast of the main taxiway of CAAF, first identified through borings and delay-time analysis of refraction data, was imaged using refraction tomography. Seismic velocity tomograms along two lines imaged this feature, which is at a depth of approximately 25–30 m, with geophysical dimensions 75–250-m wide by about 5–10-m deep. Combining the tomographic results with other refraction and borehole data reveals a trough or elongate filled doline trending approximately east-west, becoming broader to the east. The western part of this feature is associated with high rates of contaminant vapor extraction, suggesting contaminants in the unconsolidated overburden may be concentrated over this feature. This buried depression should be investigated further, since its deeper sections could contain solutionally enlarged fractures that would allow contaminants to migrate to the upper or lower aquifers.

Acknowledgments We would like to thank the US Army Environmental Center (AEC), for funding the initial stages of this work, and Mr. Wayne Mandell of the AEC for facilitating this funding. We would also like to thank an anonymous reviewer for comments and suggestions that greatly improved our manuscript.

References

- ADL (1997) Hydrogeologic Report: RCRA SMWU Assessment and RCRA Facility Investigation of Sites at Fort Campbell, Kentucky, vols. 1 and 2, Arthur D. Little, Inc., Cambridge, MA, reference no. 67072–01
- Carey, MJ (1990) The delineation of karst drainage to identify possible contamination migration routes from the Campbell Army Airfield, Fort Campbell, Kentucky. MS Thesis, 60 p., Eastern Kentucky University, Richmond
- Carpenter PJ, Higuera-Diaz IC, Thompson MD, Atre S, Mandell W (2003) Accuracy of seismic refraction tomography codes at karst sites. In: SAGEEP2003: symposium on the application of geophysics to engineering and environmental problems, environmental and engineering geophysical society, Wheat Ridge, Co., pp 832–840 (CD-ROM)
- Carpenter PJ, Breuer E, Higuera-Diaz IC, Thompson MD, Sheehan J, Doll WE, Mandell W (2004) Seismic tomographic imaging of buried karst features. In: SAGEEP2004: symposium on the application of geophysics to engineering and environmental problems, Environmental and Engineering Geophysical Society, Wheat Ridge, CO., 1114–1124 (CD-ROM)
- Dames and Moore, Inc. (1988) Boring log for CAAF-8A, 22 July 1988
- Dames and Moore, Inc. (1989) Boring log for B-2, 15 June 1989
- EWC (1989) Ft. Campbell groundwater study. Final report: submitted to USATHAMA by Ewers RO, Carey MC, Green DL (eds) Ewers Water Consultants, Inc., Richmond
- EWC (1994) Data recorded at Boiling Spring, Blue Spring, Quarles Spring, Campbell Army Airfield Well, MCI-2, and Little West Fork Creek—Ft. Campbell Kentucky: final report prepared by Ewers, RO, Idstein PJ, and Burns JL (eds) for the US Army Environmental Center, Ewers Water Consultants, Inc., Richmond
- EWC (1997) Dye tracing studies related to solid waste management units 1,2,3,4,5,6,15,28,140, and 146, Ft. Campbell, Kentucky: Ewers Water Consultants Inc., Richmond, KY, 32 p
- GeoTomo LLC (2002) GeoCT-II, Version 2.3: Advanced imaging technologies for geophysical engineering applications, users guide and codes, GeoTomo LLC, Houston
- Haeni FP, Grantham DG and Ellefesen K (1987) Microcomputer-based version of SIPT—a program for the interpretation of seismic-refraction data (text and diskettes). In: US Geological Survey open file report 87–103-A, 33 p
- Kemmerly PR (1976) Definitive doline characteristics in the Clarksville quadrangle, Tennessee. *Geol Soc Am Bull* 87:42–46
- Klemic H (1966) Geologic map of the oak grove quadrangle, Kentucky–Tennessee. US Geological Survey map GQ-565
- Padar CA (1998) Assessment of the hydrogeologic framework beneath Campbell Army Airfield, Fort Campbell, Kentucky, using geophysical techniques. MS Thesis, Northern Illinois University, DeKalb, 77 p
- Sheehan JR, Doll WE, Mandell WA (2005) An evaluation of methods and available software for seismic refraction tomography analysis. *J Environ Eng Geophys* 10:21–34
- STEP (2001) Data Summary for Phase IV Campbell Army Airfield RCRA RFI for Free Product Recovery at Pumphouse 1, Pumphouse 2, Monitoring Wells CAAF-7, CAAF-11, CAAF-14, CAAF-32, Abandoned Fuel Line, and AOC-D, Fort Campbell, Kentucky, report submitted to the US Army Corps of Engineers, Nashville District by Solutions to Environmental Problems (STEP), Inc., 88 p
- Thompson MD (1999) Geophysical investigation of the Blivet Repair Facility, Ft. Campbell, Kentucky, Argonne National Laboratory internal report, Energy Systems Division, 13 p
- Thompson MD, Cooper J, Miller SF and Mandell WA (1999) Geophysical surveys near the Fuel Storage Site, Campbell Army Airfield, Fort Campbell, Kentucky. In: Argonne National Laboratory report GWS99, 26 p
- Thompson MD (2003) Seismic tomography code meeting, Energy Systems Division, Argonne National Laboratory Technical Memo, 12 March 2003, 9 p
- Zhang J, Toksöz MN (1998) Nonlinear refraction traveltimes tomography. *Geophysics* 63:1726–1737